

# Modified SCA Algorithm for SSSC Damping Controller Design in Power System

**Bidyadhar Rout<sup>\*1</sup>, B.B. Pati<sup>\*2</sup>, and S. Panda<sup>\*3</sup>, Non-members**

## ABSTRACT

This paper studies the improvement of transient stability of a Single-Machine Infinite-Bus (SMIB) power system using Proportional Derivative (PD) type Static Synchronous Series Compensator (SSSC) and Power System Stabilizer (PSS) damping controllers. The design problem has been considered as optimization problem and a modified version of recently proposed Sine Cosine Algorithm (SCA) has been employed to determine the optimal controller parameters. Proposed modified SCA (mSCA) algorithm is first tested using bench mark test functions and compared with original SCA, and other heuristic evolutionary optimization algorithms like Grey Wolf optimization (GWO), Particle Swarm Optimization (PSO), Gravitational Search algorithm (GSA) and Differential Evolution algorithm to show its superiority. The proposed mSCA algorithm is then applied to optimize simultaneously the parameters of PD type SSSC and PSS damping controller. The performances of the proposed controllers are evaluated in SMIB power system subjected to various severe disturbances. To show the effectiveness and robustness of the proposed design approach, simulation results are presented and compared with conventional lead lag SSSC and PSS damping controller. It is observed that significant improved results are obtained with proposed mSCA algorithm compared to original SCA, GWO, PSO, GSA and DE algorithms. It is also noticed that proposed PD type SSSC and PSS controller exhibits a superior damping performance compared to conventional lead lag structured SSSC and PSS damping controllers.

**Keywords:** Sine and cosine algorithm, Lead lag controller, SSSC, PSS, Proportional Derivative Controller, Transient Stability.

## 1. INTRODUCTION

Low frequency electromechanical oscillations are observed in power systems during transient disturbances as well as because of interconnection of power systems through weak tie lines. Power systems may

lose its stability and eventually collapses from rest of the healthy systems if sufficient measures are not taken to damping these oscillations [1]. Power System Stabilizers (PSS) are now regularly employed by utilities to damp low frequency oscillations [2-4]. Due to its simplicity and reliability, the lead lag structure PSS is mostly designed in linear model but is limited to off line power systems [5-6]. Conventional techniques for designing PSS may not improve the system damping in a large scale power systems containing very large number of controllers of improper co-ordinations. The difficulties in designing of PSS are simplified in time domain and frequency domain by intelligent optimisation based technique [7-15].

Nevertheless, PSS alone may not provide sufficient damping for increasing line loading over long distances and inter-area power swings; in such situation other effective options are required to damp power system oscillations. Flexible AC Transmission System (FACTS) controllers especially the Static Synchronous Series Compensator (SSSC) are very effective in damping the power system oscillations [4, 16]. The FACTS controllers with PSS considerably improves the stability in a very fast manner by damping out the oscillations and also control the power transfer capacity of the power system networks [17]. SSSC is one such member of FACTS family employing a self-commutated voltage-source switching converter and is installed in series with the line. Controlling of real power and impedance in steady state by suitable model of SSSC is proposed in [18-19]. The dynamic stability uses an auxiliary stabilizing signal with SSSC to improve power system stability [20]. The synchronizing torque, damping torque and transient stability limit for both small signal as well as transient stability are effectively improved with real power as input to the lead-lag (LL) based SSSC damping controller as reported in [21]. The transient stability enhancement power system oscillation damping with SSSC are reported in several references [22-25]. The coordination between existing PSS and incorporating of FACTS family members improve the overall system performances employing power oscillation damping controllers has been discussed in [26-32].

With adaptive or variable structure techniques, the lead-lag compensation type control structure is popularly used and compared with classical controllers because of its simple online tuning [20, 33]. This lead lag controller which is the supplementary damping controller with SSSC improves in damping out of the

Manuscript received on November 27, 2017 ; revised on February 10, 2018.

\*The authors are with Department of Electrical Engg. Veer Surendra Sai University of Technology, Burla, Odisha, India, E-mail : rout.bdr@gmail.com<sup>1</sup>, 2bbpati\_ee@vssut<sup>2</sup>, panda\_sidhartha@rediffmail.com<sup>3</sup>

oscillation and thereby improves stability. While substantial work has been proposed for controller structure of PID controller, astonishingly, barely any effort has been made to develop the structure of a lead lag controller which consists of a gain block which performances as a proportion gain and there is possibility to add an additional derivative gain term to improve the effectiveness of the controller. Therefore, a PD-type SSSC and PSS damping controller is proposed in the present work to damp power system oscillations.

Designing of PSSs and or FACTS - based controllers have been reported with pole placement method [34-36], Eigen-values sensitivities [37], residue compensation [38] etc. However, due to heavy computational burden, more time consumption, slow convergence and moreover, the controller parameters are trapped to their local minima and not optimal, the conventional methods are not desirable for robust stability. Due to the promising superiority of optimization in very complex multimodal search spaces, "Heuristics from Nature", algorithm techniques are used popularly in non-differentiable objective functions. These approaches include PSO [24, 30-31], GA [29], DE [32, 39], multi-objective evolutionary algorithm (MOGA) [40] etc. Sine Cosine Algorithm (SCA) is a recently proposed optimization technique which is based on the well-known sine and cosine functions in which several random and adaptive variables are integrated for exploration and exploitation capability in the search space [41]. The superiority of SCA algorithm over Firefly Algorithm (FA) and such other algorithms has been reported in literature [42].

This paper proposes a modified version of SCA to further improve the exploration and exploitation capability of the algorithm. To improve overall system performance, the parameters of PD type SSSC and PSS damping controllers are simultaneously optimized by proposed modified SCA algorithm. To show the robustness of the proposed design approach, simulation results are presented less than three phase disturbance at different operating conditions and fault location for a single-machine infinite-bus power system.

## 2. SYSTEM INVESTIGATED

### 2.1 Single Machine Infinite Bus Power System with SSSC

To assess the robustness of damping performances the co-ordinately designed controllers are tested in a SMIB system depicted in Fig. 1. The system contains a synchronous generator connected to an infinite-bus through a double circuit (DC) transmission line. The generator is provided with SSSC, Hydraulic Turbine and Governor (HTG) and excitation system along with Power system stabilizer. The HTG consists of a hydraulic turbine, a governor system, and a servomotor. The excitation system consists of a voltage regulator and dc exciter, as recommended in IEEE

Recommended Practice for Excitation System Models for Power System Stability Studies [43]. In Fig.1, the SSSC is connected in series in between bus1 and bus2 through coupling transformer. A line transformer  $T$  links to the generator and bus1; Bus2 and bus3 are connected through DC transmission line and bus3 to infinite bus [1].  $V_T$  And  $V_B$  are the generator terminal and infinite-bus voltages respectively;  $V_1$  and  $V_2$  are the bus voltages at bus1 and bus2 respectively as shown. Current  $I$  is the line current,  $P_{L1}$  is the real power flowing in one of the double circuit transmission line and  $P_L$  is the tie line active power flows in transmission line. The proposed model of power system shown in Fig. 1 is developed using Sim Power Systems block set [43]. All the relevant parameters are given in appendix.

### 2.2 Structure of SSSC and Control System

SSSC consist of a three-phase voltage source converter (VSC), a series coupling transformer, a dc capacitor  $V_{dc}$ , and AC and DC voltage regulator. The objective of using voltage source converter is to converts a dc voltage into sinusoidal three phase AC voltage with fundamental frequency which is to be injected into line and quadrature (independent from line current) with the line current  $I$ . The injected AC voltage  $V_q$  changed its magnitude due to variable fictitious capacitive or inductive reactance during transient condition. This voltage controls the active power flow efficiently and damps out the power swings [17]. In capacitive mode,  $V_{cnv}$  is greater than  $V_{ac}$  and it supplies active and reactive power to power system and in inductive mode,  $V_{cnv}$  is lower than  $V_{ac}$ , SSSC consumes power. The control device maintains the voltage profile of transmission line unchanged by controlling the converter voltage [16]. The control structure of SSSC is of the reactance scheme-based controller in capacitive mode is shown in Fig. 2 comprises of a phase-locked loop (PLL), AC and dc voltage regulator, voltage and current measuring units, and pulse width modulator (PWM) for controlling voltage source converter (VSC). Bus voltage  $V_1$  and  $V_2$  through potential transformer and line current  $I$  through current transformer are measured. PLL is used to generate the reference angle  $\theta$  which is phase locked to phase of the voltage at bus#1. The stator current  $I_d$  and  $I_q$  in synchronous reference frame are calculated using reference angle  $\theta$  of PLL. The reactance produced during oscillation is multiplied by the current magnitude  $I$  to obtain required compensated voltage magnitude. The required  $V_{dcref}$  is determined from this compensated voltage. The actual dc voltage  $V_{dc}$  is compared with  $V_{dcref}$  and the error is passed through proportional integral (PI) controller of dc voltage regulator to produce  $V_{dcnv}$ . The  $V_q$  voltage regulator known as AC voltage regulator is a PI type controller requires only  $I_d$  component neglecting  $I_q$ .  $V_{qref}$  represents the reference in-

jected voltage desired by steady state power flow and assumed to be constant in large disturbance. The change of SSSC injected voltage  $\Delta V_q$  compares with the reference  $V_{qref}$  and passed through AC regulator which generates  $V_{qcnv}$ . The combined effect of  $V_{dcnv}$  and  $V_{qcnv}$  results the converter voltage  $V_q$  through PWM technique which is to be injected to the transmission line required for voltage compensation and control of active power.

### 2.3 Dynamic Modeling of Synchronous Generator during Transient Stability

The single machine infinite bus model has several classifications of dynamic time scales and each classification is represented by a set of dynamic equations. In the present paper, the dynamic modeling of synchronous generator is done in synchronous ( $d-q$ ) reference frame. The machine consists of stator winding in  $d$ - and  $q$ -axis, rotor winding in  $d$ -axis and three short circuited damper windings (one in  $d$ -axis and others two in  $q$ -axis). All rotor parameters are referred to stator by primed variables as given in Eqs. (1) - (8).

$$V_d = R_s i_d + \frac{d}{dt} \phi_q - \omega_R \phi_q \quad (1)$$

$$V_d = R_s i_q + \frac{d}{dt} \varphi_q - \omega_R \phi_d \quad (2)$$

$$V'_{fd} = R'_{fd} i'_{fd} + \frac{d}{dt} \varphi'_{fd} \quad (3)$$

$$V'_{kd} = R'_{kd} i'_{kd} + \frac{d}{dt} \varphi'_{kd} \quad (4)$$

$$V'_{kq1} = R'_{kq1} i'_{kq1} + \frac{d}{dt} \varphi'_{kq1} \quad (5)$$

$$V'_{kq2} = R'_{kq2} i'_{kq2} + \frac{d}{dt} \varphi'_{kq2} \quad (6)$$

Where,

$$\varphi_d = L_d i_d + L_{md} (i'_{fd} + i'_{kd}),$$

$$\varphi_q = L_q i_q + L_{mq} i'_{kq},$$

$$\varphi'_{fd} = L'_{fd} i'_{fd} + L_{md} (i_d + i'_{kd}),$$

$$\varphi'_{kd} = L'_{kd} i'_{kd} + L_{md} (i_d + i'_{fd}),$$

$$\varphi'_{kq1} = L'_{kq1} i'_{kq1} + L_{mq} i_q,$$

$$\varphi'_{kq2} = L'_{kq2} i'_{kq2} + L_{mq} i_q,$$

Where,  $d$  and  $q$  represents  $d$ -axis and  $q$ -axis quantities,  $R$  and  $S$  represents rotor and stator quantities,  $f$  and  $k$  represents field and damper winding,  $l$  and  $m$  represents leakage and magnetizing inductance.

The mechanical equations are given by:

$$\frac{d}{dt} \omega_r = \frac{1}{J} (P_e - B\omega_r - P_m) \quad (7)$$

$$\frac{d}{dt} \theta = \omega_r \quad (8)$$

Where  $\omega_r$  and  $\theta$  represents the mechanical state variables of the generator  $P_e$  and  $P_m$  are the electrical output and mechanical input power respectively,  $J$  and  $B$  represent inertia and viscous friction of rotor respectively.

### 2.4 Control Structures of PD type SSSC and PSS Damping Controller

A PD type SSSC and PD type PSS are the design part of the control structure shown in Fig. 3 and Fig. 4 respectively. The proposed PD type SSSC and PSS is a supplementary damping controller whose structure is shown in Fig. 3, is to modulate the SSSC injected voltage  $V_q$ . The proposed control structure have a proportional gain  $K_p$  and a derivative gain block  $K_d$  with two stage lead lag compensator block. The compensation block consists of a washout block which serves as a high pass filter with time constant  $T_W$  is used to ensure that there is no steady-state error of the voltage reference due to the speed deviation  $\Delta w$ . Time constant  $T_W$  is not critical and may be in the range of 1 to 20 sec [2]. In the proposed test system  $T_W = 10$ s is taken into consideration. The phase compensation block provides the phase lead characteristics to compensate for phase lag between the input and output signal. Further, with addition of lead lag compensator in PSS structure, the required poles and zeroes are placed at its desired location of s-plane that improves the transient and overshoot of the responses. The performances are also improved by derivative block as far as no sharp corner of input signal is concerned and it results an unreasonable size control inputs to the plant when sharp corners signal of input is injected to the derivative block. This limits the practical application of derivative controller and can be avoided by putting a first order filter with tuning pole and the chattering due to noise are eliminated. As the input signal (i.e.  $\Delta w$ ) to the controller is remote signal, the sensor time with transmission time delay  $T_{TD} = 65$  ms is provided at the input to the PD type SSSC controller and only sensor time delay  $T_{td} = 15$  ms is provided for PD type PSS controller. The filter constant is taken as filter gain of proposed PD type SSSC controller. The structure of PD type PSS is shown in Fig. 4. A first order sensor with sensor time delay  $T_{td} = 15$  ms is chosen with this controller for sensing the low frequency speed deviation  $\Delta w$  during disturbances. The function of PD type PSS is to provide a damping electrical torque which is in phase with speed deviation during low frequency oscillation. With taking the speed deviation  $\Delta w$  as input the structure generates the stabilising voltage

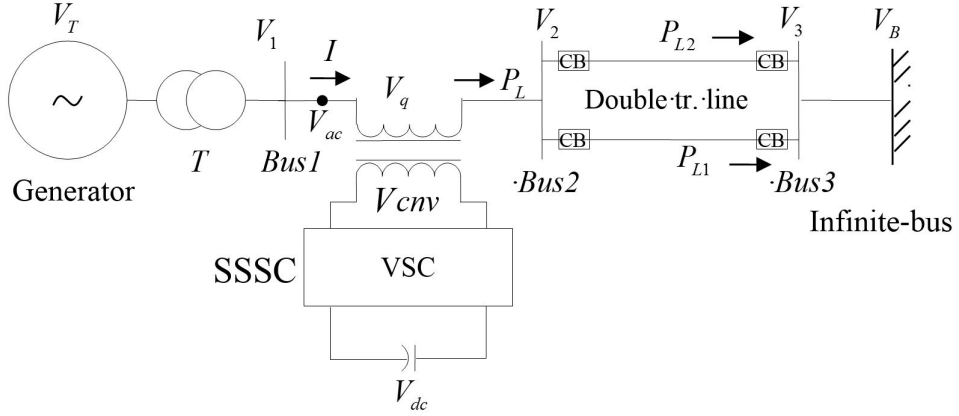


**Fig. 1:** The Single Machine Infinite Bus (SMIB) Power System with a SSSC

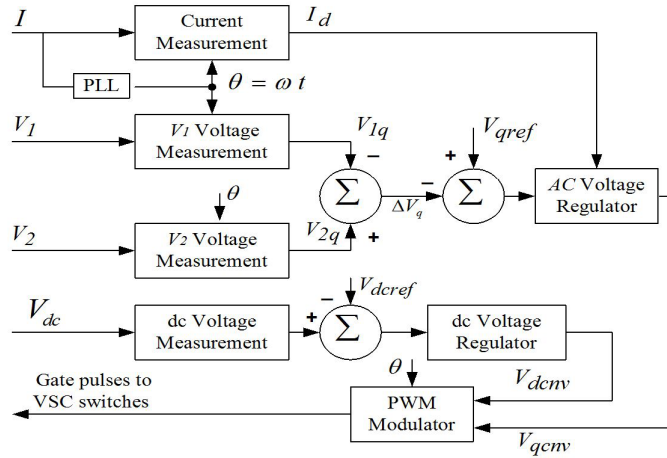


**Fig. 2:** The Control structure of SSSC

as output which is given to the voltage regulator of excitation system to produce the required field voltage and damped out the oscillation maintaining the terminal voltage constant. In the present paper the advantage of proposed PD type SSSC and PSS structures over conventional lead lag structures have been demonstrated. The structures of conventional lead lag SSSC and PSS damping controllers are shown in Fig. 5 and Fig. 6 respectively

## 2.5 Controller Models

The output voltage signal obtained from different control structure is as follows:

For proposed PD type SSSC and PSS damping controller,

$$U_{SSSCP} = \left( \frac{1}{0.065s + 2} \right) \left( K_d \frac{sN}{s + N} + K_p \right) \times \left( \frac{sT_W}{1 + sT_W} \right) \left( \frac{1 + sT_1}{1 + sT_2} \right) \left( \frac{1 + sT_3}{1 + sT_{41}} \right) y \quad (9)$$

For PD type PSS

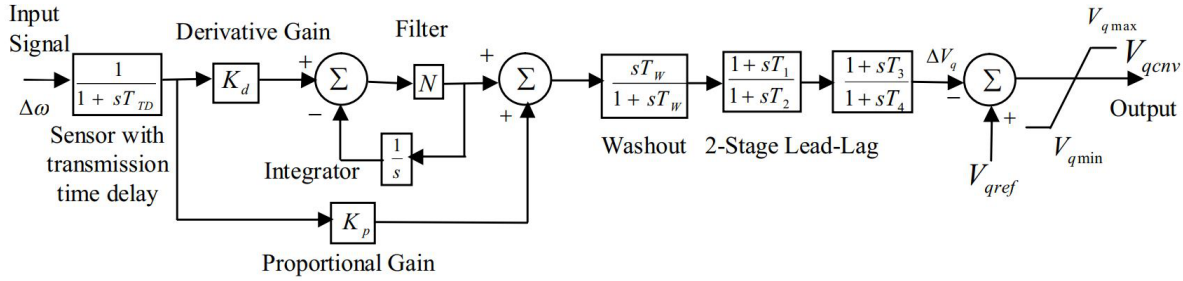
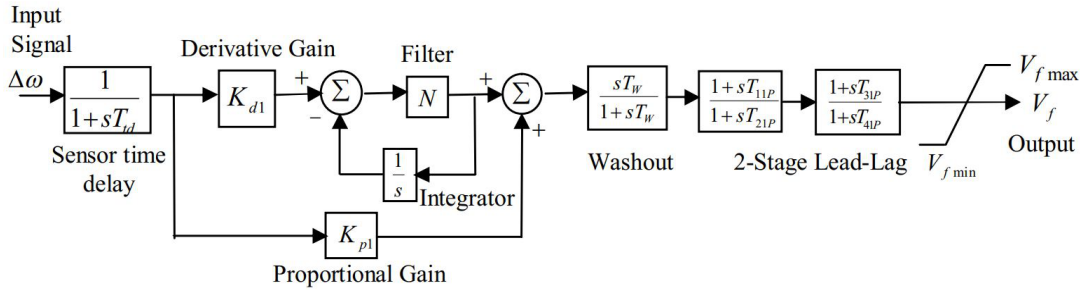
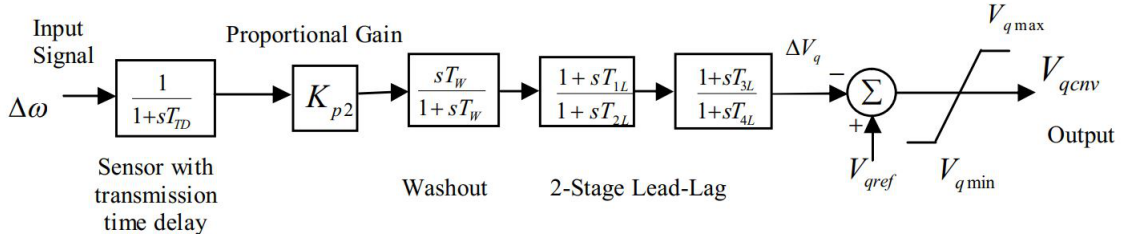
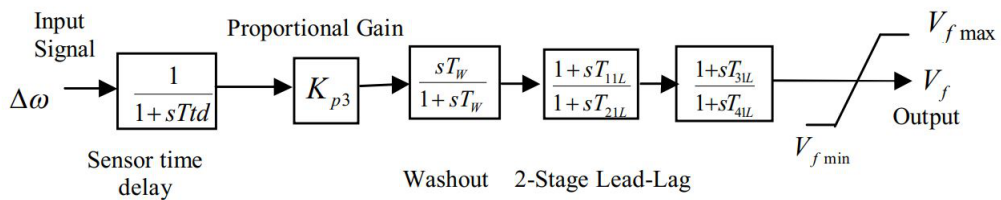
$$U_{PSSP} = \left( \frac{1}{0.015s + 1} \right) \left( K_{d1} \frac{sN}{s + N} + K_{p1} \right) \times \left( \frac{sT_W}{1 + sT_W} \right) \left( \frac{1 + sT_{11p}}{1 + sT_{21p}} \right) \left( \frac{1 + sT_{31p}}{1 + sT_{41p}} \right) y \quad (10)$$

For Lead Lag SSSC and PSS controller

$$U_{SSSCL} = \left( \frac{1}{0.065s + 1} \right) K_{p2} \left( \frac{sT_W}{1 + sT_W} \right) \times \left( \frac{1 + sT_{1L}}{1 + sT_{2L}} \right) \left( \frac{1 + sT_{3L}}{1 + sT_{4L}} \right) y \quad (11)$$

For Lead Lag PSS

$$U_{PSSL} = \left( \frac{1}{0.015s + 1} \right) K_{p3} \left( \frac{sT_W}{1 + sT_W} \right) \times \left( \frac{1 + sT_{11L}}{1 + sT_{21L}} \right) \left( \frac{1 + sT_{31L}}{1 + sT_{41L}} \right) y \quad (12)$$

**Fig.3:** Structure of PD type SSSC and PSS damping controller**Fig.4:** Structure of PD type PSS**Fig.5:** Structure of Lead Lag SSSC and PSS controller**Fig.6:** Structure of excitation based Lead Lag PSS

Where  $K_p$ ,  $K_d$ ,  $K_{p1}$ ,  $K_{d1}$ ,  $T_1$ ,  $T_2$ ,  $T_3$ ,  $T_4$ ,  $T_{11P}$ ,  $T_{21P}$ ,  $T_{31P}$ ,  $T_{41P}$  are gains and time constant parameters of PD type SSSC-PSS and PD type PSS controller must be tuned for achieving stabilizer's best performances. Similarly,  $K_{p2}$ ,  $K_{p3}$ ,  $T_{1L}$ ,  $T_{2L}$ ,  $T_{3L}$ ,  $T_{4L}$ ,  $T_{11L}$ ,  $T_{21L}$ ,  $T_{3L}$  and  $T_{4L}$  are the gain and time constant parameters of lead-lag SSSC-PSS and lead-lag PSS must be optimally tuned to compare the performances of the responses with proposed PD type SSSC controller.

In this proposed system the speed deviation  $\Delta\omega$  is

taken as input signal  $y$  in all controllers as input i.e. the change in speed  $\Delta\omega$  which is sensitive to more participation factor, easily controllable and observable for local mode oscillation.

## 2.6 Control Objectives

The control objective (single objective is taken) is to minimize only the speed deviation  $\Delta\omega$  so that, the system oscillations are damped out during post fault condition and enhances the power system stability. However, both electromechanical and electro-

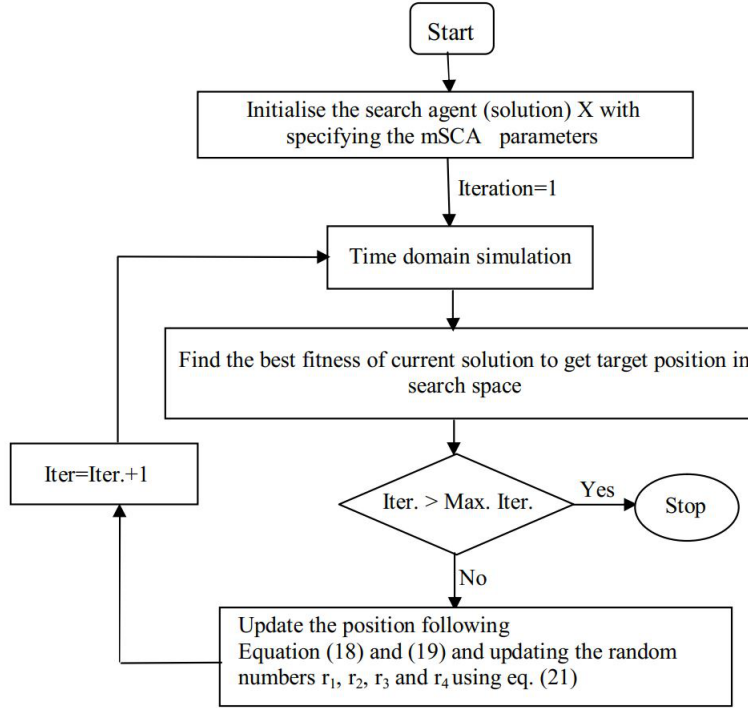


**Fig.7:** Flow chart of mSCA algorithm.

magnetic oscillations are seen in rotor speed deviation, rotor angle and tie line power of transmission system respectively. These oscillations do not allow the desired power flow in transmission line which leads to instability if oscillation persists for long duration. Minimization of any of one or all (multi objective functions) could be chosen as objective function. Since the speed deviation  $\Delta w$  is a local mode signal, it is considered as objective function for the proposed system.

The minimization of the objective function improves the system transient response in terms of the overshoots, rise time and settling time subjected to constraints of designed controller parameters.

The objective function for SMIB is:

$$J = \int_{t=0}^{t=t_{sim}} |\Delta w(t)| t dt \quad (13)$$

Where,  $t_{sim}$  is time range of the simulation,  $\Delta w(t)$  is the speed deviation, the performance indices Integral of Time weighted Absolute value of Error (ITAE) is chosen as objective function which is to be minimized. The objective function of system model is calculated in simulation time. The deviation of objective function changes with respect to change in controller parameters. However, the minimization of objective function  $J$  is subjected to constraint of controller parameters. Minimize  $J$

Subjected to: (PD type SSSC based damping controller)

$$\begin{aligned} K_p^{\min} \leq K_p \leq K_p^{\max}, K_d^{\min} \leq K_d \leq K_d^{\max}, \\ T_1^{\min} \leq T_1 \leq T_1^{\max}, T_2^{\min} \leq T_2 \leq T_2^{\max}, \\ T_3^{\min} \leq T_3 \leq T_3^{\max}, T_4^{\min} \leq T_4 \leq T_4^{\max} \end{aligned} \quad (14)$$

(PD type PSS controller):

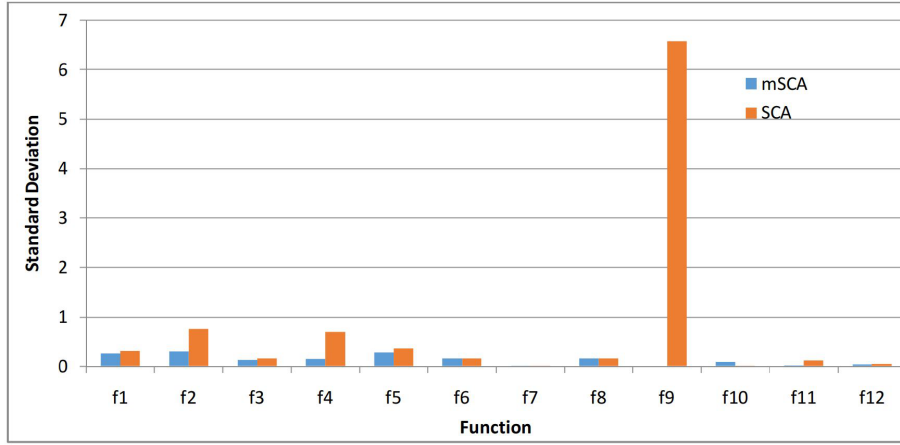
$$\begin{aligned} K_{p1}^{\min} \leq K_{p1} \leq K_{p1}^{\max}, K_{d1}^{\min} \leq K_{d1} \leq K_{d1}^{\max}, \\ T_{11P}^{\min} \leq T_{11P} \leq T_{11P}^{\max}, T_{21P}^{\min} \leq T_{21P} \leq T_{21P}^{\max}, \\ T_{31P}^{\min} \leq T_{31P} \leq T_{31P}^{\max}, T_{41P}^{\min} \leq T_{41P} \leq T_{41P}^{\max} \end{aligned} \quad (15)$$

(PD type PSS controller):

$$\begin{aligned} K_{p2}^{\min} \leq K_{p2} \leq K_{p2}^{\max} \\ T_{1L}^{\min} \leq T_{1L} \leq T_{1L}^{\max}, T_{2L}^{\min} \leq T_{2L} \leq T_{2L}^{\max}, \\ T_{3L}^{\min} \leq T_{3L} \leq T_{3L}^{\max}, T_{4L}^{\min} \leq T_{4L} \leq T_{4L}^{\max} \end{aligned} \quad (16)$$

(LL type PSS controller):

$$\begin{aligned} K_{p3}^{\min} \leq K_{p3} \leq K_{p3}^{\max} \\ T_{11L}^{\min} \leq T_{11L} \leq T_{11L}^{\max}, T_{21L}^{\min} \leq T_{21L} \leq T_{21L}^{\max} \\ T_{31L}^{\min} \leq T_{31L} \leq T_{31L}^{\max}, T_{41L}^{\min} \leq T_{41L} \leq T_{41L}^{\max} \end{aligned} \quad (17)$$

**Fig.8:** Comparison of standard deviation of mSCA with SCA**Table 1:** Unimodal benchmark functions

Types	Function	Dim.	Range	$f_{min}$
Unimodal	$f_1(x) = \sum_{i=1}^n x_i^2$	30	[-100,100]	0
	$f_2(x) = \sum_{i=1}^n  x_i  + \prod_{i=1}^n  x_i $	30	[-10,10]	0
	$f_3(x) = \sum_{i=1}^n \left( \sum_{j=1}^i x_j \right)^2$	30	[-100,100]	0
	$f_4(x) = \max_i \{ x_i , 1 \leq i \leq n\}$	30	[-100,100]	0
	$f_5(x) = \sum_{i=1}^{n-1} [100(x_{i+1} - x_i^2) + (x_i - 1)^2]$	30	[-30,30]	0
	$f_6(x) = \sum_{i=1}^n (x_i + 0.5)^2$	30	[-100,100]	0
	$f_7(x) = \sum_{i=1}^n i x_i^4 + \text{random}(0, 1)$	30	[-1.28,1.28]	0

**Table 2:** Multimodal Function

Types	Function	Dim.	Range	$f_{min}$
multimodal	$f_8(x) = \sum_{i=1}^n -x_i \sin(\sqrt{ x_i })$	30	[-500,500]	$-418.9829 \times 5$
	$f_9(x) = \sum_{i=1}^n [x_i^2 - 10 \cos(2\pi x_i) + 10]$	30	[-5.12,5.12]	0
	$f_{10}(x) = -20 \exp \left( -0.2 \sqrt{\frac{1}{n} \sum_{i=1}^n x_i^2} \right) - \exp \left( \frac{1}{n} \sum_{i=1}^n \cos(2\pi x_i) \right) + 20 + e$	30	[-32,32]	0
	$f_{11}(x) = \frac{1}{4000} \sum_{i=1}^n x_i^2 - \prod_{i=1}^n \cos \left( \frac{x_i}{\sqrt{i}} \right) + 1$	30	[-600,600]	0
	$f_{12}(x) = \frac{\pi}{n} \left\{ 10 \sin(\pi y_1) + \sum_{i=1}^{n-1} (y_i - 1)^2 [1 + 10 \sin^2(\pi y_{i+1})] + (y_n - 1)^2 \right\} + \sum_{i=1}^n u(x_i, 10, 100, 4)$ $y_i = 1 + \frac{x_i + 1}{4}$ $u(x_i, a, k, m) = \begin{cases} k(x_i - a)^m x_i > a \\ 0 - a < x_i < a \\ k(-x_i - a)^m x_i < -a \end{cases}$			

### 3. OVERVIEW OF ALGORITHM

#### 3.1 Sine Cosine Algorithm [41] and its modification:

Population based algorithm selects the global optimal values and avoids the local optima in all real challenging problems in contrast to individual based algorithm. Sine and Cosine algorithm (SCA) is a recently new developed optimization technique whose algorithm is based on sine and cosine mathematical functions. The global optimal solution is obtained after several iteration steps with large number of random solutions. Optimization of this algorithm undergoes into two phases. In the exploration phase a promising region is formed by an optimization algorithm with the random solutions in the solution set at high rate while in the exploitation phase, the change of random solutions and random variation is slow and global optima is obtained. The mathematical modelling of sin and cosine algorithm is shown by the updating positions of solution for both phases is represented by

$$X_j^{t+1} = X_j^t + r_1 \times \sin(r_2) \times |r_3 P_j^t - X_j^t| \quad (18)$$

When  $r_4 < 0.5$

$$X_j^{t+1} = X_j^t + r_1 \times \cos(r_2) \times |r_3 P_j^t - X_j^t| \quad (19)$$

When  $r_4 \geq 0.5$

Where  $X_j^{t+1}$  updating position of next solution in  $j$ th dimension at  $t$ -th iteration,  $X_j^t$  position of current solution,  $P_j^t$  is the target position in  $j$ th dimension,  $r_1/r_2/r_3/r_4$  are the main parameters of SCA and are random numbers in the range  $[0, 1]$ . The random number implies the next position's (movement) region which could be inside or outside the solution space,  $r_2$  leads the movement of position for a solution is towards or outwards the target destination. The number  $r_3$  is the random weight supports to the destination position  $P_j^t$  emphasizing the distance if  $r_3 > 1$  and not emphasizing for  $r_3 < 1$ . The random number  $r_4$  selects the sine and cosine components depending on the number. If  $r_4 < 0.5$ , the update position enters into sine domain and if  $r_4 \geq 0.5$ , the position enters into cosine domain.

The update position inside and outside can be extended by changing the range  $(-2, 2)$  of sine and cosine functions and the random location inside and outside the region is possible for  $r_2$  in  $(0, 2\pi)$  as reported in [41]. To obtain the promising region and global optimum in search space, the exploration and exploitation must be balanced by the sine and cosine algorithm which is done by changing  $r_1$  in the equation (18) and (19) as

$$r_1 = a - t \left( \frac{a}{T} \right) \quad (20)$$

Where,  $a = \text{constant}$ ,  $t = \text{current iteration}$  and  $T = \text{maximum number of iteration}$ .

Further, to improve the convergence and global optima, SCA algorithm is extended by modifying the random number  $r_1$  which is implemented in this proposed work. The random number  $r_1$  for mSCA is given by

$$r_1 = a - t^2 \left( \frac{a}{T^2} \right) \quad (21)$$

Where constant  $a = 1.6$ , the iteration  $t$  is changed to its fractional power of 2, the maximum number of iteration  $T$  is changed to its fractional power value of 2, in equation (21) as  $r_1$  satisfies the line equation following nonlinear path to find its optimum solutions. Moreover, this mSCA is well tested in various benchmark functions [42] which is compared with few optimization techniques mentioned in table 3 and table 4. Some satisfactory results are obtained on average value and standard deviation using mSCA. This motivates the proposed mSCA for implementation in proposed power system. The flow chart of mSCA algorithm is depicted in Fig. 7

#### 3.2 Benchmark Test Functions [42]:

A set of benchmark function for unimodal and multimodal [42] is considered in table 1 and table 2. Each of the benchmark function shows  $f_{min}$  as zero after 30 runs in a particular range. However, these functions are validated in table 3 and table 4 through several optimizing techniques and proposed optimizing algorithm to show their effectiveness in terms of  $f_{min}$  as standard deviations. In the current study, the performance analysis of modified SCA algorithm was carried out by fitting to some standard benchmark functions. The benchmark functions include some unimodal and some multimodal function as these functions prove the exploration and exploitation capability of the algorithm and used by many researchers. These functions expressions, dimensions (Dim), ranges and optimum solutions ( $f_{min}$ ) are given in the Table 1 and 2. After implementing the proposed algorithm to the benchmark functions, the obtained results are compared with original SCA and also with some recent meta-heuristic techniques like GWO, PSO, GSA and DE. The statistical results like average and standard deviations are arranged in the Table 3 and 4. While performing the test the search agents are chosen as 30, maximum number of iterations are taken as 500 and the algorithm is made to run for 30 as proposed in the original SCA. In all population based algorithms, the optimization process is divided in to two conflicting stages: exploration and exploitation. Exploration encourages potential solutions to change abruptly and stochastically thus improving the diversity of the solutions. On the other hand, exploitation aims for improving the quality of solutions by searching locally around

**Table 3:** Comparison of average and standard deviation of uni-modal function ( $f$ ) with proposed mSCA

$f$	GWO[42]		PSO[42]		GSA[42]	
	Ave	Std. Dev	Ave	Std. Dev	Ave	Std. Dev
$f_1$	6.59E-28	6.34E-05	0.000136	0.000202	2.32E-16	9.67E-17
$f_2$	7.18E-17	0.029014	0.042144	0.045421	0.055655	0.194074
$f_3$	3.29E-17	79.14958	70.12562	22.11924	896.537	318.9559
$f_4$	5.61E-07	1.315088	1.086481	0.317039	7.35487	1.741452
$f_5$	26.81258	69.9049	96.71832	60.11559	67.54309	62.225534
$f_6$	0.816579	0.00012	0.000102	8.28E-05	2.5E-16	1.74E-16
$f_7$	0.002213	0.10028	0.122854	0.044957	0.089441	0.04339
$f$	DE[42]		SCA		mSCA	
	Ave	Std. Dev	Ave	Std. Dev	Ave	Std. Dev
$f_1$	8.2E-14	5.9E-14	2.48E-11	0.3085	1.043E-33	0.2607
$f_2$	1.5E-09	9.9E-10	3.133E-10	0.7500	1.085E-19	0.2926
$f_3$	6.8E-11	7.4E-11	0.0392	0.1579	5.43E-25	0.1248
$f_4$	0	0	5.623E-04	0.7007	3.03E-23	0.1486
$f_5$	0	0	7.8396	0.3628	7.3395	0.2734
$f_6$	0	0	0.7048	0.1611	0.4795	0.1532
$f_7$	0.00463	0.0012	0.0027	0.0028	1.490E-4	0.0017

**Table 4:** Comparison of average and standard deviation of multimodal function ( $f$ ) with proposed mSCA

$f$	GWO[42]		PSO[42]		GSA[42]	
	Ave	Std. Dev	Ave	Std. Dev	Ave	Std. Dev
$f_8$	-6123.1	-4087.44	-4841.29	1152.82	2821.07	493.0375
$f_9$	0.310521	47.35612	46.70423	11.62938	25.96841	7.470068
$f_{10}$	1.06E-13	0.07783	0.276015	0.50901	0.62087	0.23628
$f_{11}$	0.004485	0.006659	1.009215	0.007724	27.70154	5.040343
$f_{12}$	0.053438	0.020734	0.006917	1.799617	0.95114	7.95114
$f$	DE[42]		SCA		mSCA	
	Ave	Std. Dev	Ave	Std. Dev	Ave	Std. Dev
$f_8$	-11090.1	574.7	-2.1506E+03	0.1532	-1.956E+03	0.1534
$f_9$	69.2	38.8	2.4377	6.5691	0	0
$f_{10}$	9.7E-08	4.2E-08	0.0011	0.0058	1.125E-15	0.0901
$f_{11}$	0	0	0.0762	0.1183	0.0042	0.0231
$f_{12}$	7.9E-15	8E-15	0.1689	0.0495	0.1008	0.0383

**Table 5:** Optimized parameters with objective function

Controllers	Parameters (optimized with mSCA )						ITAE *10e - 3
	$K_p$	$K_d$	$T_1$	$T_2$	$T_3$	$T_4$	
PD type SSSC and PSS	61.7418	0.1142	0.0137	0.8762	1.4653	0.0013	2.7
	0.9990	0.3723	0.0056	0.0290	0.0553	0.7532	
Lead Lag SSSC and PSS	$K_{p2}$	-	$T_{1L}$	$T_{2L}$	$T_{3L}$	$T_{4L}$	4.5
	40.7360	-	0.2523	0.4713	1.6030	1.4317	
Lead Lag PSS	$K_{p3}$	-	$T_{11L}$	$T_{21L}$	$T_{31L}$	$T_{41L}$	4.5
	12.0203	-	0.7586	1.2281	1.9468	1.0112	

**Table 6:** Optimized parameters with objective function

Controllers	Optimiz. Tech.	Optimized Parameters						ITAE *10e-3
		$K_p$	$K_d$	$T_1$	$T_2$	$T_3$	$T_4$	
PD type SSSC and PSS	<b>mSCA</b>	<b>61.7418</b>	<b>0.1142</b>	<b>0.0137</b>	<b>0.8762</b>	<b>1.4653</b>	<b>0.0013</b>	<b>1.9</b>
	SCA	259.6578	40.6458	1.2523	1.0301	1.0125	1.9974	
PD type PSS	<b>mSCA</b>	$K_{p1}$	$K_{d1}$	$T_{11p}$	$T_{21p}$	$T_{31p}$	$T_{41p}$	<b>1.9</b>
		<b>0.9990</b>	<b>0.3723</b>	<b>0.0056</b>	<b>0.0290</b>	<b>0.0553</b>	<b>0.7532</b>	
	SCA	30.4044	40.6458	0.1550	1.9974	0.1873	0.0010	2.7

the obtained promising solutions in the exploration stage. In original SCA, the transition between exploration and exploitation is generated by the component which decreases linearly as given in Eq. (20). Better exploration of search space may result in getting stuck in local optima as too much exploration introduces randomness. To enhance the exploration rate, exponential functions are used to decrease the component as given in Eq. (21).

It is clear from Tables 3 and 4 that proposed modified SCA gives significantly improved results compared to original SCA, GWO, PSO, GSA and DE algorithms. As unimodal functions are suitable for testing exploitation capability of the algorithms, therefore, the results given in Table 3 gives evidence of high exploitation capability of the proposed modified SCA algorithm. At the same time, multimodal functions have large number of local optima. Results given in Table 4 show that proposed modified SCA algorithm is able to explore the search space extensively and find promising regions of the search space. In addition, high local optima avoidance of this algorithm is another finding that can be inferred from these results.

### 3.3 Comparison of standard deviation of mSCA with SCA

The standard deviations for benchmark functions from table3 and table4 are taken. The comparison is done between using SCA and proposed mSCA and

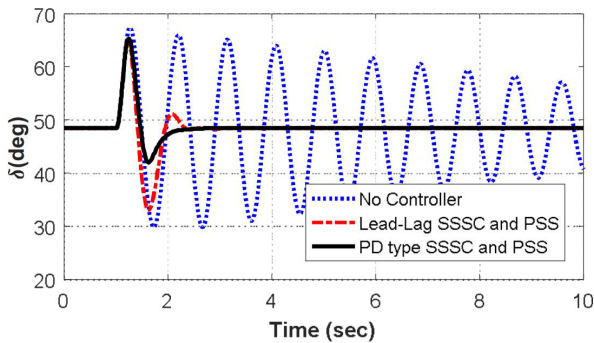
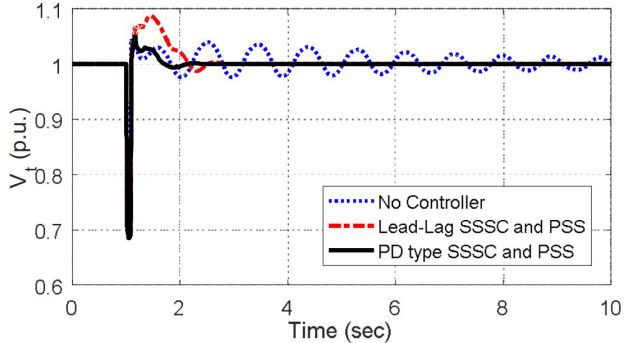
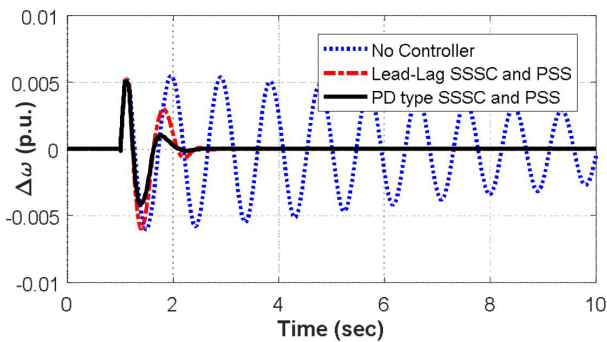
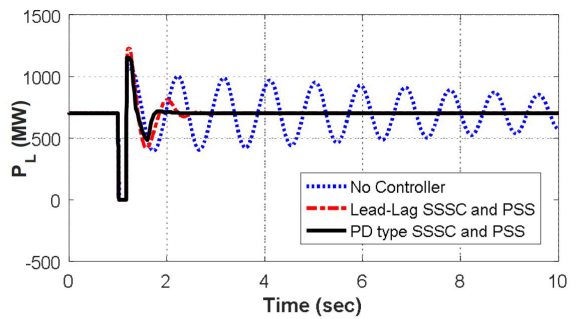
it is found that, the proposed mSCA has minimum value of standard deviations which is shown in Fig. 8. Since the error must have the minimum value of standard deviation to converge, the proposed mSCA is better than the SCA for implementation in proposed system.

### 3.4 Application of mSCA technique to optimize the controller parameters

To further investigate the superiority of the proposed mSCA algorithm it is applied to tune the parameters of PD type SSSC and PSS controllers. The model of the system under study has been developed using Sim Power System Toolbox in MATLAB/SIMULINK environment. For objective function calculation; the developed model is simulated in a separate programme (by .m file using initial population/controller parameters) considering a severe disturbance. Form the SIMULINK model the objective function value is evaluated and moved to workspace. The process is repeated for each individual in the population. For objective function calculation, a 3-phase short-circuit fault in one of the parallel transmission lines is considered. Using the objective function values, the population is modified by mSCA for the next generation. The optimized controller parameters are provided in Table 5. For comparison mSCA optimized lead lag SSSC and PSS parameters are also provided in Table 5.

**Table 7:** Optimized tuned parameters of mSCA, DE and WGO for comparison study

Controllers	Optimizing	Optimized Parameters						ITAE *10e-3
		$K_p$	$K_d$	$T_1$	$T_2$	$T_3$	$T_4$	
PD type SSSC and PSS	mSCA	<b>61.7418</b>	<b>0.1142</b>	<b>0.0137</b>	<b>0.8762</b>	<b>1.4653</b>	<b>0.0013</b>	<b>1.9</b>
	WGO	109.1944	1.7257	1.6109	1.1459	0.8174	1.9705	
	DE	204.3137	44.9293	0.8327	1.3603	0.0720	0.3562	
PD type PSS	mSCA	$K_{p1}$	$K_{d1}$	$T_{11p}$	$T_{21p}$	$T_{31p}$	$T_{41p}$	<b>1.9</b>
		<b>0.9990</b>	<b>0.3723</b>	<b>0.0056</b>	<b>0.0290</b>	<b>0.0553</b>	<b>0.7532</b>	
	WGO	27.0549	6.5073	0.3533	1.8290	0.5529	1.3440	3.1
	DE	10.2970	6.2598	0.3771	0.9309	0.3436	1.0422	3.0

**Fig.9:** Power angle  $\delta$ **Fig.11:** Injected terminal voltage  $V_t$ **Fig.10:** Speed deviation  $\Delta\omega$ **Fig.12:** Injected power flow  $P_L$ 

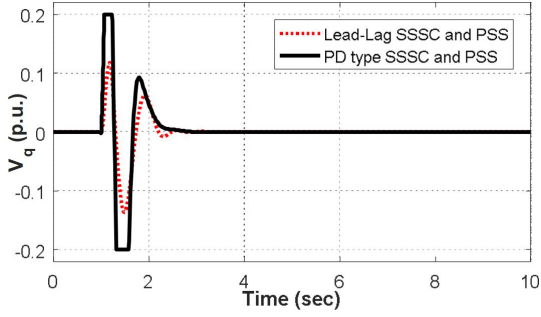
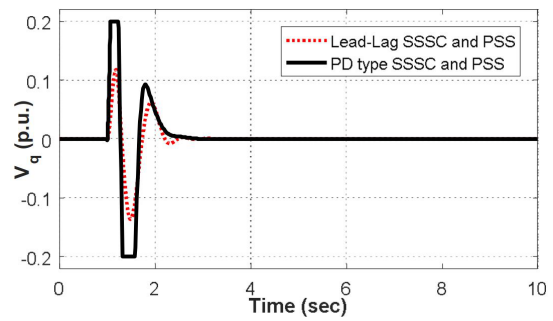
#### 4. CASE STUDY AND SIMULATION RESULTS

Different case studies are taken for nominal loadings of SMIB and the robustness and effectiveness of the responses are verified with the proposed PD type SSSC controller.

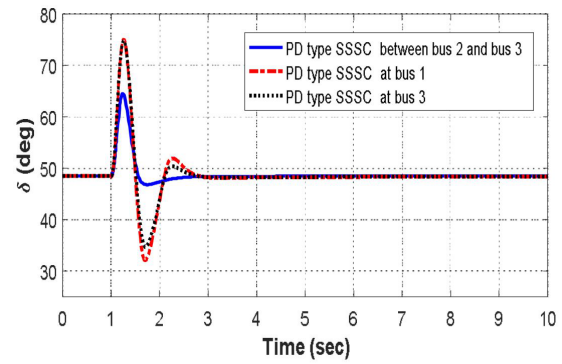
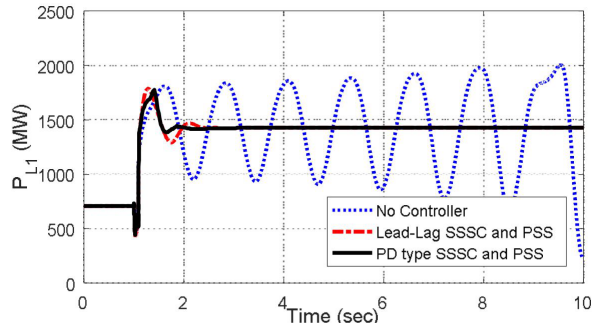
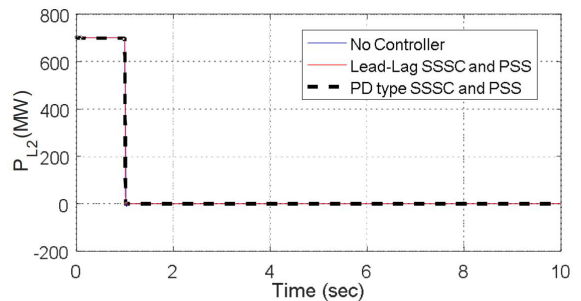
##### 4.1 Case-1 : Nominal Loading, ( $P_e = 0.8$ , $\delta_0 = 48.4^\circ$ ), line outage

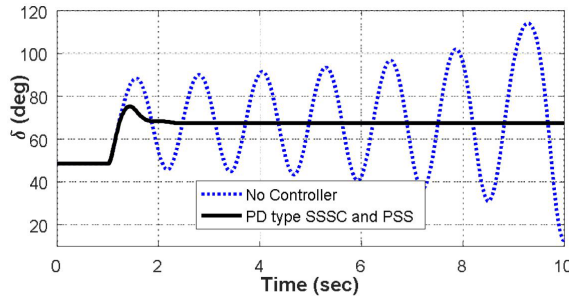
A 3-phase fault is applied for nominal loading at one of the double transmission line between bus 2 and bus 3 at  $t = 1$  sec and line outage for 5 cycles

(0.084 sec). The mechanical oscillations of generator shaft position (rotor angle) and velocity (speed deviation) with respect to their reference position and electromagnetic oscillation of bus terminal voltage, active power in tie line, injected voltage and field voltages are observed in Fig.9 to Fig.15 respectively during post fault conditions. To make the power flow and maintaining the system voltages steady the oscillations are damped out using PD type SSSC damping controller with its coordinated PD type PSS in excitation system. Fig.9 shows the rotor angle behavior in degree using proposed controller and compared with no controller and lead lag type SSSC controller. It is seen that, the proposed controller brings the ro-

**Fig. 13:** SSSC-injected voltage  $V_q$ **Fig. 14:** Effect of excitation field voltage  $V_f$ 

tor angle position to its initial position of  $48.4^\circ$  just after the first swing, first overshoot and settles the oscillation at 2.0 sec. Fig. 10 shows the speed deviation (difference between reference and synchronous) in p.u. and its transient response dies out very quickly and settles at 2.0 sec. Fig. 11 results terminal voltage  $V_t$  in transmission line whose magnitude reduces during fault at 1 sec and when reclosed at 5 cycles it restores to its equilibrium point at 1 p.u. through modulated SSSC injected voltage  $V_q$  without much increasing in its magnitude from unity. As terminal voltage reduces during fault, the corresponding active power decreases following  $P_L = \frac{V_t E}{x} \sin \delta$  where,  $V_t$  is terminal voltage,  $E$  is the excitation emf in generator,  $x$  is the reactance of whole power systems and  $\delta$  is the rotor angle. The response of active power is shown in Fig. 12 in which it is clear that, the rotor gains kinetic energy during fault that increases the rotor angle for which the electromagnetic torque and hence power developed and increases much high in first swing and then decreases. The proposed controller brings the power to its operating point after 2 sec. and maintains to flow. SSSC injected voltage  $V_q$  response is shown in the Fig. 13 which explains that, before fault, the SSSC generates  $V_q=0$ , and it injects  $V_q$  with limiting to 0.2 p.u. during transient period to compensate the terminal voltage  $V_t$ . The terminal voltage increases following increase of power in voltage stability region. The excitation system of the synchronous generator generates the large field voltage due to sudden change in current and presence of high inductive field coil during three phase fault. It is seen in the Fig. 14 that; the field voltage is increased around 7 times from its nominal value. For this reason, the ceiling voltage of field system is kept around much high of its rated field voltage. Further, the proposed PD type SSSC and PSS damping controller is tested at various bus positions in SMIB by applying three phase fault with selfclearing. It is shown in Fig. 15 that, the rotor angle is peakier at first swing for bus 1 as it is nearer to generator in comparison to bus 3 and in between (bus 2 and bus 3) and the proposed controller settles the bus 1 response more effectively at 2.8 sec as same as other bus settling time.

**Fig. 15:** Effect of power angle  $\delta$  at various bus positions**Fig. 16:** Power Flow in healthy line  $P_{L1}$ **Fig. 17:** Power Flow in Faulty line  $P_{L2}$

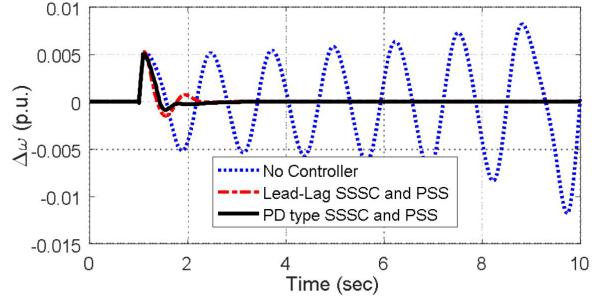
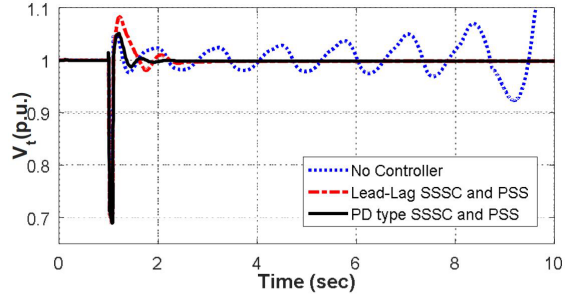
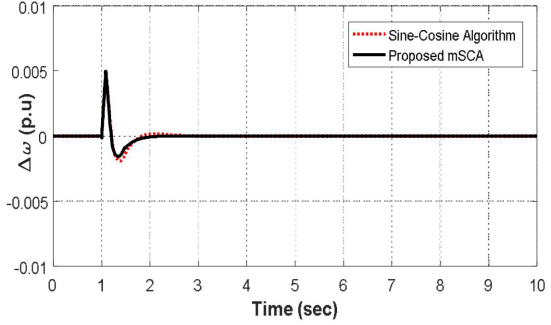
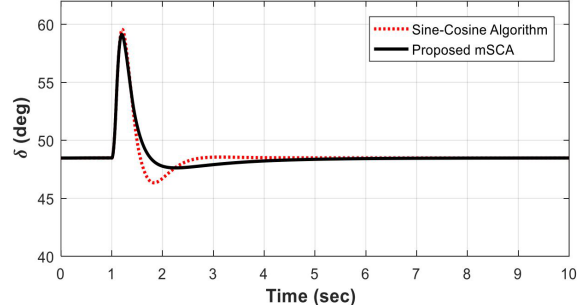
Fig. 18: Effect of power angle  $\delta$ 

#### 4.2 Case-2 : Nominal Loading, ( $P_e = 0.8, \delta_0 = 48.4^\circ$ ) with Permanent line tripping

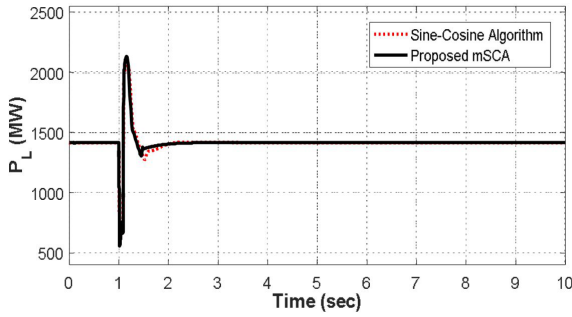
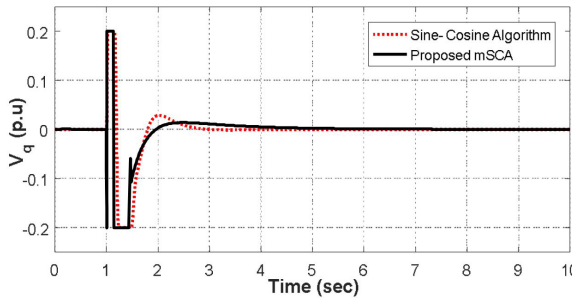
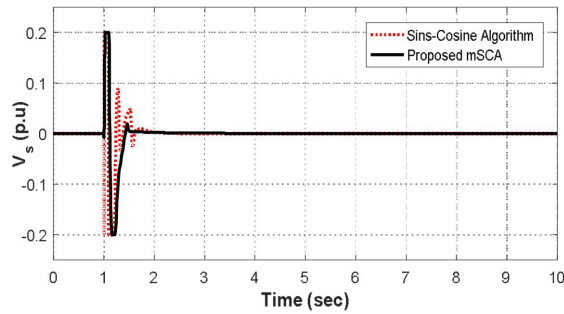
The proposed controller is also tested in nominal loading with permanent line tripping. The three phase fault is created at one of the line between the bus#2 and bus#3 at 1 sec. The fault is cleared after 5 cycles from occurrence of fault and the concerned faulted line is permanently disconnected from the existing double circuit. All the system responses are shown from (Fig. 16 to Fig. 20). It is observed from these figures that, due to tripping of one of the double circuit line, the line reactance increases and hence reduces the active power. As the mechanical power is constant, the electrical power will maintain its steady value of 1417 MW which will flow in the healthy part of double circuit line which is shown in Fig. 16. The initial power in healthy line  $L_1$  was 707 MW, when fault occurs at line  $L_2$  and disconnected permanently, the power flows in healthy line is now increased to 1417MW due to absence of other line  $L_2$ . In faulty line, no power  $P_{L2}$  will flow due to permanently disconnected and is shown in Fig. 17. The rotor angle accordingly increases to  $67.5^\circ$  from its initial value of  $48.4^\circ$  due to absence of one of the double circuit line shown in Fig. 18. The proposed controller damps out the rotor oscillation without first swing and settles angle  $67.5^\circ$  at 2.3 sec. This shows the effectiveness and robustness of the proposed controller. The speed deviation and the terminal voltages are shown in Fig. 19 and Fig. 20 respectively and the significant damping is observed with reduced settling time. In all the response cases, the system becomes unstable without controller and the proposed controller stabilizes the system more effectively than lead lag SSSC and PSS controller.

#### 4.3 Case-3 : (Comparison of SCA with mSCA) for SMIB with nominal loading ( $P_e = 0.8, \delta_0 = 48.4^\circ$ )

The simulation results are compared for original SCA with modified SCA on same nominal loading conditions for SMIB power system. It is observed from Fig. 21 to Fig. 25 that, the overshoot and undershoot of all responses are improved in mSCA

Fig. 19: Effect of speed deviation  $\Delta w$ Fig. 20: Injected terminal voltage  $V_t$ Fig. 21: Speed deviation  $\Delta w$ Fig. 22: Power angle  $\delta w$ 

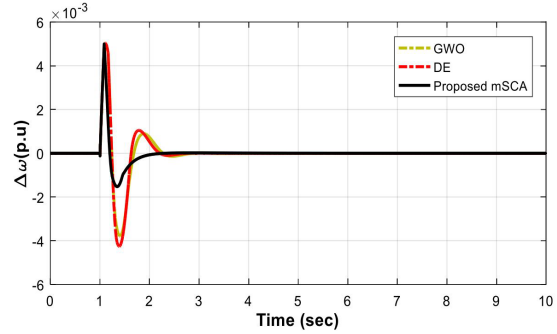
in comparison to original SCA by modifying the line equation using the proposed PD type SSSC based damping controller. This shows the effectiveness of the modified mSCA techniques over SCA algorithm. Table6 shows the optimizing controller parameters of

**Fig.23:** Injected power flow  $P_L$ **Fig.24:** SSSC-injected voltage  $V_q$ **Fig.25:** Stabilizing voltage  $V_s$ 

SCA and mSCA with their ITAE value.

#### 4.4 Case-4 : (Comparison mSCA with DE, WGO optimization technique) for SMIB with nominal loading ( $P_e = 0.8, \delta_0 = 48.4^\circ$ )

The effectiveness of the proposed using mSCA is also compared with DE and GWO optimization technique is shown in table7 and result in Fig. 26. All controller parameters optimally tuned by above mentioned algorithms and the results are shown in table7. Simulation result for speed deviation is taken from all three algorithms in Fig. 26 and it is found that, mSCA optimization technique gives more effective response than DE and GWO at same nominal loading conditions for SMIB power system.

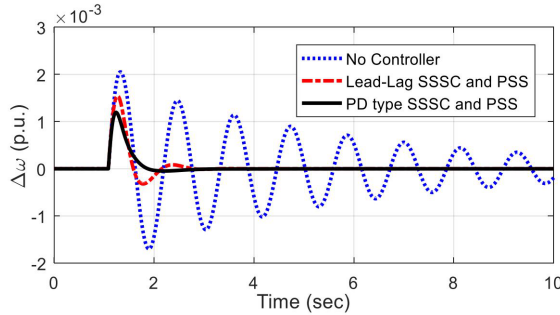
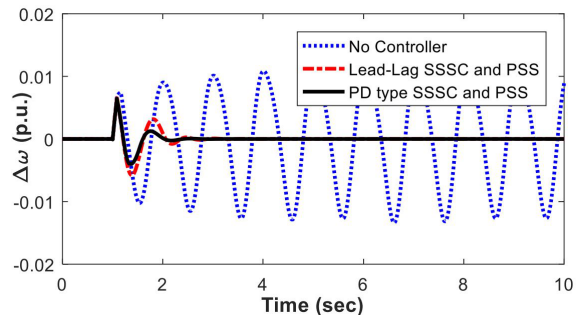
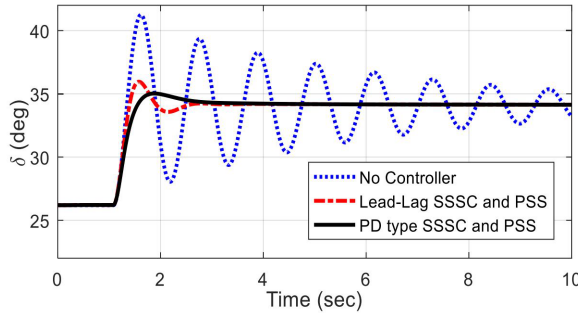
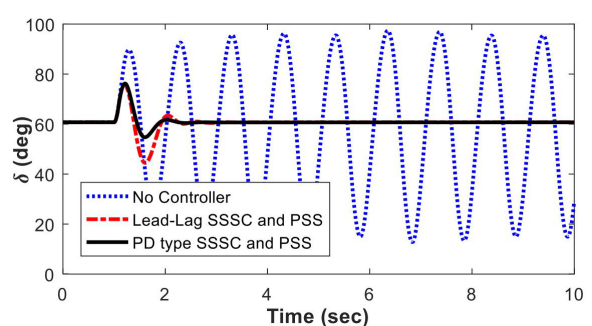
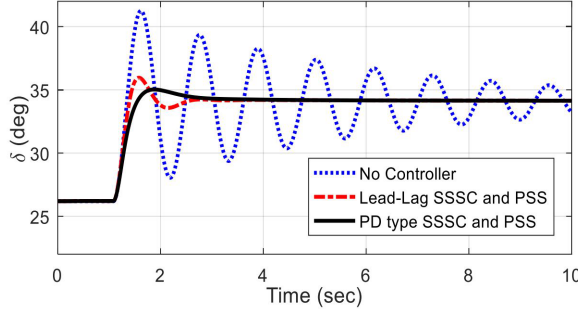
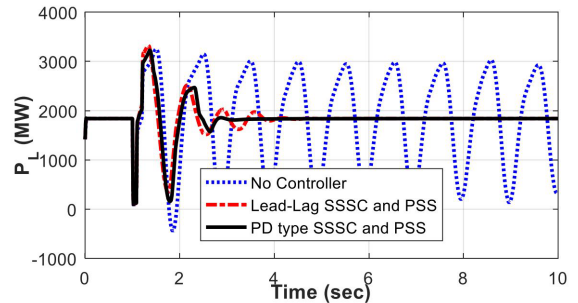
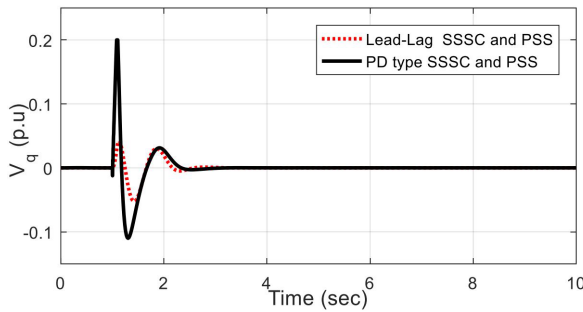
**Fig.26:** speed deviation  $\Delta\omega$  for mSCA, DE and GWO

#### 4.5 Case-5 : Light Loading, $P_e = 0.45, \delta_0 = 26.2^\circ$ self-clearing

The robustness is verified at light loading with 3 phase fault applied near bus3 at  $t = 1$  s and self-cleared after 5 cycles. The system speed deviation, power angle, line power and SSSC injected voltage are depicted in Fig. 27, 28, 29 and Fig. 30 respectively. The speed deviation response is very quickly damped out with PD type SSSC and PSS controller as compared with lead lag SSSC and PSS controller which are shown in Fig. 27. The overshoot as well as settling time is reduced in this proposed controller as compared with lead-lag SSSC and PSS controller. With the light load, the rotor angle increases from its reference angle  $26.2^\circ$  and settles at  $34.3^\circ$  after 5 cycles following three phase fault at bus 3. Proposed controller settles the new position of the rotor angle at  $34.3^\circ$  and is shown in Fig. 28. The overshoot is reduced and settles without second overshoot. However, the rise time is poor as compared to the lead-lag SSSC and PSS controller. The effectiveness of tie power flow response is shown in Fig. 29. The nominal power of 1417 MW is reduced to 620 MW at 0.45p.u. light loading and then three phase disturbance is applied at bus 3. Unlike lead lag SSSC and PSS, the proposed controller damps out the tie power response more effectively and settles it at 620 MW. Response in Fig. 30 shows the SSSC injected voltage to the transmission line during faulty period to compensate the reduced terminal voltage. However, the maximum and minimum limit of the SSSC injected voltage of (+ 0.2 p.u to -0.2 p.u) is considered in the simulation work. All simulation results in light load conditions shows the effectiveness of the proposed PD type SSSC and PSS controller in this proposed SMIB system.

#### 4.6 Case-6 : Heavy Loading, ( $P_e = 1, \delta = 60.02^\circ$ ), temporary load tripping

The operating condition is changed with heavy loading where  $P_e = 1, \delta_0 = 60.02^\circ$  in this proposed SMIB system. The three phase fault is ap-

Fig. 27: Speed deviation  $\Delta\omega$ Fig. 31: Speed deviation  $\Delta\omega$ Fig. 28: Power angle  $\delta$ Fig. 32: Speed deviation  $\delta$ Fig. 29: Injected power flow  $P_L$ Fig. 33: Injected power flow  $P_L$ Fig. 30: Injected voltage  $V_q$ 

plied at bus3 and the load is removed temporarily for 200ms. The system responses becomes sustained oscillatory during three phase disturbance at heavy loading condition. The proposed PD type SSSC and PSS improves the damping more effectively and the sta-

bility is maintained. The robustness and effectiveness of the proposed controller is verified for various responses. The system responses of speed deviation, rotor angle and tie line power are shown in the Fig. 31, Fig. 32 and Fig. 33 respectively. The damping of speed response reduces the overshoot and undershoots as shown in Fig. 31. The initial rotor angle is 60.020 at heavy load as shown in Fig. 32. The angle settles at 60.020 after the post fault period. The transient response is reduced with the proposed controller. The tie line power also increases to 1850 MW from nominal value of 1417 MW in heavy loading and during transient period it increases to 2880MW and reduces to 1850 MW by the proposed controller as shown in Fig. 33. The stability of SMIB is maintained by the proposed PD type SSSC and PSS damping controller with more effective manner.

## 5. CONCLUSION

This work presents a design of the coordinated controller of PD type SSSC and PSS damping controller and PD type PSS on SMIB power systems. The controller parameters are tuned optimally through modified SCA algorithm (derived from recently developed novel SCA algorithm) and implemented in the controller of the proposed power systems in order to minimize the objective function during post fault condition. The robustness and the effectiveness for the designed controller whose parameters are tuned through mSCA are verified through the system responses. Further, the robustness of the proposed PD type SSSC and PSS controller is compared with lead lag SSSC and PSS controller at different operating condition and different fault locations for the proposed power systems and it is found that, the coordinated PD type SSSC and PSS damping controller gives effective result in system time domain responses through its overshoots, rise time and settling time and provides stabilization by enhancing the damping and brings the system responses to its equilibrium points. Comparison between the SCA and mSCA has been performed and such responses are shown from which the effectiveness of the mSCA is observed. The mSCA algorithm is also compared with DE and GWO population based algorithm and better results for controller parameters are obtained from proposed mSCA. The superiority of mSCA than GWO and DE is shown in the simulation results. All Simulation works are done on MATLAB environment. It is concluded that, the proposed algorithm can also be implemented in multi machines and multi area power systems.

## 6. ACKNOWLEDGMENT

The authors would like to thank for using the facilities created in VSSUT out of AICTE sponsored RPS Project entitled “Transient Stability Analysis and Control of Power Systems with Excitation Control” -2012

## 7. REFERENCES

### References

- [1] P. M. Anderson and A. A. Fouad, *Power System Control and Stability*, Ames, IA: Iowa State Univ. Press, 1977, ch.1.
- [2] P. Kundur, *Power System Stability and Control*, McGraw-Hill, 1994, ch.12.
- [3] P. Kundur, J. Paserba, V. Ajjarapu, G. Andersson, A. Bose, C. Canizares, N. Hatziargyriou, D. Hill, A. Stankovic, C. Taylor, T. VaCutsem, and V. Vittal, “Definition and classification of power system stability,” *IEEE Trans. Power Syst.*, vol. 19, no. 2, pp. 1387-1401, May. 2004.
- [4] F. D. DeMello and C. Concordia, “Concepts of synchronous machine stability as affected by excitation control,” *IEEE Trans. Power App. Syst.*, Vol. PAS-88, no.2, pp. 316-329, Apr. 1969.
- [5] T. Hussein, M. S. Saad, A. L. Elshafei and A. Bahgat, “Damping inter-area modes of oscillation using an adaptive fuzzy power system stabilizer,” *Electr. Power Syst. Res.*, Vol. 80, no. 12, pp. 1428-1436, 2010.
- [6] H. J. Chow, E. G. Boukarim and A. Murdoch, “Power system stabilizer as undergraduate control design project,” *IEEE Trans. Power Syst.*, Vol.19, no. 1, pp.144-151, 2004.
- [7] H. Yassami, A. Darabi and S. M. R. Rafiei, “Power system stabilizer design using Strength Pareto multi-objective optimization approach,” *Electr. Power Syst. Res.*, Vol. 80, pp. 838-846; 2010.
- [8] Y. L. Abdel-Magid and M. A. Abido, “Optimal multi-objective design of robust power system stabilizers using genetic algorithms,” *IEEE Trans. Power Syst.*, Vol. 18, pp. 1125-1132, 2003.
- [9] S. Mishra, M. Tripathy and J. Nanda, “Multi-machine power system stabilizer design by rule based bacteria foraging,” *Electr. Power Syst. Res.*, Vol.77, pp. 1595-1607, 2007.
- [10] M. A. Abido, “Robust design of multi-machine power system stabilizers using simulated annealing,” *IEEE Trans. Energy Conv.*, Vol.15, pp. 297-304, 2000.
- [11] M. A. Abido and Y. L. Abdel-Magid, “Robust design of multi-machine power system stabilizers using tabu search algorithm,” *IEE Proc.-Gener. Transf. Distribut*, Vol. 147, pp. 387-94, 2000.
- [12] P. Zhang and A. H. Coonick, “Coordinated synthesis of PSS parameters in multi-machine power systems using the method of inequalities applied to genetic algorithms,” *IEEE Trans. Power Syst.*, Vol. 15, pp. 811-816, 2000.
- [13] E. R. C. Viveros, G. N. Taranto and D. M. Falco, “Coordinated tuning of AVR and PSSs by multi-objective genetic algorithms,” *13th Int. conference intell. syst. applicat. power syst.*, pp. 247-252, 2005.
- [14] T. T. Nguyen and R. Giusto, “Optimal design for control coordination of power system stabilizers and flexible alternating current transmission system devices with controller saturation limits,” *IET Gener. Transm. Distrib*, Vol. 4, no. 9, pp. 1028-43, 2010.
- [15] R. A. , B. C. Pal, N. Martins and J. C. R. Ferraz, “Robust and coordinated tuning of power system stabilizer gains using sequential linear programming,” *IET Gener. Trans. Distrib*, Vol. 4, no. 8, pp. 893-904, 2010.
- [16] R. M. Mathur and R. K. Varma, *Thyristor-based FACTS controllers for electrical transmission systems*, John Wiley and Sons, Inc., New York: Springer, 2005, ch.10
- [17] N.G. Hingorani and L. Gyugyi, *Understanding*

**APPENDIX** System data [43]

SMIB	Generators	$S_B = 2100MVA, H = 3.7s, V_B = 13.8KV, f = 60Hz, X_d = 1.305, X_d' = 0.296, X_d'' = 0.252, X_q = 0.474, X_q' = 0.243, X_q'' = 0.18, T_d = 1.01s, T_d' = 0.053s, T_{qo}' = 0.1s, P_e = 1680MW$
	Load	Load = 250 MW
	Transformer	$S_{BT} = 2100MVA, D_1/Y_g connection, 13.8/500KV, f = 60Hz, R_1 = R_2 = 0.002\Omega, L_1 = 0, L_2 = 0.12H, R_m = 500\Omega, L_m = 500H$
	Transmission lines	$3-phase, f = 60Hz, L_1 = 30km, L_{2-1} = 150km, L_{2-2} = 150km, R_1 = 0.02546\Omega/km, R_0 = 0.3864\Omega/km, L_1 = 0.9337e - 3H/km, L_0 = 4.1264e - 3H/km, C_1 = 12.74e - 9F/km, C_0 = 7.751e - 9F/km$
	Hydraulic Turbine and Governor	$K_a = 3.33, T_a = 0.07, G_{\min} = 0.01, G_{\max} = 0.97518, V_{g\min} = -0.1pu/s, V_{g\max} = 0.1pu/s, R_p = 0.05, K_p = 1.163, K_i = 0.105, K_d = 0, T_d = 0.01s, \beta = 0, T_W = 2.6/s$
	Excitation System	$T_{LP} = 0.02s, K_a = 200, T_a = 0.001s, K_e = 1, T_e = 0, T_b = 0, T_C = 0, K_f = 0.001, T_f = 0.1s, V_{f\min} = 0, V_{f\max} = 7, K_p = 0$
	SSSC	$S_{nom} = 100MVA, V_{nom} = 500KV, f = 60Hz, V_{q\max} = 0.2, \text{max rate of change } V_{qref} = 3/s, R_{cnv} = 0.00533\Omega, L_{cnv} = 0.16H, V_{DC} = 40KV, C_{DC} = 37e - 6F, K_{P\_IVR} = 0.00375, K_{I\_IVR} = 0.1875, K_{P\_VdcR} = 0.1e - 3, K_{I\_VdcR} = 20e - 3$

- FACTS: Concepts and Technology of Flexible AC Transmission Systems*, IEEE Press, New York, 2000
- [18] X. P. Zhang, "Advanced modeling of the multi-control functional static synchronous series compensator (SSSC) in Network power flow," *IEEE Trans. Power Syst.*, Vol. 18, no. 4, pp. 1410-1416, 2003.
- [19] L. Gyugyi, C. D. Schauder and K. K. Sen, "Static synchronous series compensator: a solid-state approach to the series compensation of transmission lines," *IEEE Trans. Power Del.*, Vol. 12, pp. 406-417, 1997.
- [20] H. F. Wang, "Static synchronous series compensator to damp power system oscillations," *Elect. Power Syst. Res.*, Vol. 54, pp. 113-119, 2000.
- [21] M. S. Castro, H. M. Ayres, V. F. da Costa and L. C. P. da Silva, "Impacts of the SSSC control modes on small-signal and transient stability of a power system," *Elect. Power Syst. Res.*, Vol. 77, pp. 1-9, 2007.
- [22] K. K. Sen, "SSSC-Static synchronous series compensator-Theory, modeling, and applications," *IEEE Trans. Power Del.*, vol. 13, no. 1, pp. 241-245, Jan. 1998.
- [23] S. Panda, "Multi-objective evolutionary algorithm for SSSC-based controller design," *Elect. Power Syst. Res.*, Vol. 79, pp. 937-944, 2009.
- [24] S. Panda, N.P. Padhy and R.N. Patel, "Power system stability improvement by PSO optimized SSSC-based damping controller," *Elect. Power Comp. Syst.*, Vol. 36, pp. 468-490, 2008.
- [25] S. R. Khuntia and S. Panda, "ANFIS approach for SSSC controller design for the improvement of transient stability performance," *Math. Comput. Modelling*, Vol.57, Issue 1-2, pp. 289-300, Jan. 2013.
- [26] Y. L. Abdel-Magid and M. A. Abido, "Robust co-ordinated design of excitation and TCSC-based stabilizers using genetic algorithms," *Elect. Power Energy Syst.*, Vol. 69, pp. 129-141, 2004.
- [27] J. M. Ramirez and I. Castillo, "PSS and FDS simultaneous tuning," *Elect. Power Systs. Res.*, Vol. 68, pp. 33-40, 2004.
- [28] L. J. Cai and I. Erlich, "Simultaneous coordinated tuning of PSS and FACTS damping controller in a large power system," *IEEE Trans. Power Syst.*, Vol. 20, pp. 294-300, 2005.
- [29] S. Panda and R. N. Patel, "Damping power system oscillations by genetically optimized PSS and TCSC controller," *Int. J. Energy Tech. Policy*, Vol. 5, pp. 457-474, 2007.
- [30] S. Panda, N. P. Padhy and R. N. Patel, "Robust coordinated design of PSS and TCSC using PSO technique for power system stability enhancement," *J. Elect. Syst.*, vVol. 3, pp. 109-123,

2007.

- [31] S. Panda and N.P. Padhy, "Optimal location and controller design of STATCOM using particle swarm optimization," *J. Franklin Inst.*, Vol. 345, pp. 166-181, 2008.
- [32] S. Panda, "Robust coordinated design of multiple and multi-type damping controller using differential evolution algorithm," *Int. J. Elect. Power Energy Syst.*, Vol. 33, pp. 1018-1030, 2011.
- [33] R. Mihalic and I. Papic, "Static synchronous series compensator mean for dynamic power flow control in electric power systems," *Elect. Power Syst. Res.*, Vol. 45, pp. 65-72, 1998.
- [34] P. Shrikant Rao and I. Sen, "Robust pole placement stabilizer design using linear matrix inequalities," *IEEE Trans. Power Syst.*, Vol. 15, No. 1, pp. 3035-3046, Feb. 2000.
- [35] M. A. Abido, "Pole placement technique for PSS and TCSC based stabilizer design using simulated annealing," *Int. J. Elect. Power Syst. Research*, Vol. 22, No. 8, pp. 543-554, 2000.
- [36] B. C. Pal, "Robust pole placement versus root-locus approach in the context of damping inter-area oscillations in power systems," *IEE Proc. Generation, Transmission Distribution*, Vol. 49, No. 6, pp. 739-745, 2002.
- [37] L. Rouco and F.L. Pagola, "An eigenvalue sensitivity approach to location and controller design of controllable series capacitor for damping power system oscillations," *IEEE Trans. Power Syst.*, Vol. 12, No. 4, pp. 1660-1666, 1997.
- [38] M. E. About-Ela, A. A. Sallam, J. D. Mc Calley and A. A. Fouad, "Damping controller design for power system oscillations using global signals," *IEEE Trans. Power Syst.*, Vol. 11, pp. 767-773, 1996.
- [39] S. Panda, "Differential evolution algorithm for SSSC-based damping controller design considering time delay," *J. Franklin Institute*, Vol. 348, Issue 8, pp. 1903-1926, Oct. 2011.
- [40] S. Panda, "Multi-objective non-dominated sorting genetic algorithm-II for excitation and TCSC-based controller design," *J. Elect. Eng.*, Vol. 60, pp. 87-94, 2009.
- [41] S. Mirjalili, "SCA: a sine cosine algorithm for solving optimization problems," *Knowledge Based Syst.*, Vol. 96, pp. 120-133, Mar. 2016.
- [42] S. Mirjalili, S. M. Mirjalili and A. Lewis, "Grey wolf optimizer," *Adv. Eng. Softw.*, Vol. 69, pp. 46-61, 2014.
- [43] *Sim Power Syst. 5.2.1 User's Guide*.



**Bidyadhar Rout** received his B. Tech from IGIT Sarang, India and M.Tech in control system Engineering from IIEST, W.B. India. He is currently Assistant Professor, Department of Electrical Engineering at Veer Surendra Sai University of Technology (VSSUT), Odisha, India. His areas of interests are design of Linear and Non-linear excitation controller for power system stability, soft computing application in Machine drives.



**Prof. B. B. Pati** received his BSc.Engg. degree in Electrical Engineering VSSUT, Odisha. M. Tech in Power system Engineering from Indian Institute of Science, Bangalore, India and Ph.D. in Control System Engineering from Utkal University, Odisha, India. He is currently a professor in Department of Electrical Engineering in VSSUT, Odisha, India. His research interest include in Control System Engineering. He has more than hundred international journal papers to his credit. Dr. Pati is a Fellow of Institution of Engineers (India).



**Prof. S. Panda** received Ph.D. degree from Indian Institute of Technology (IIT), Roorkee, India, M.E. degree from Veer Surendra Sai University of Technology (VSSUT). Presently, he is working as a Professor in the Department of Electrical Engineering, VSSUT, Odisha, India. His areas of research include Flexible AC Transmission Systems (FACTS), Power System Stability, Soft computing, Distributed Generation and Wind Energy. He has more than hundred international journal papers to his credit. Dr. Panda is a Fellow of Institution of Engineers (India).